Analytica Chimica Acta 1157 (2021) 338396

Contents lists available at ScienceDirect

Analytica Chimica Acta

journal homepage: www.elsevier.com/locate/aca

A novel electrochemical biosensor for exosomal microRNA-181 detection based on a catalytic hairpin assembly circuit

Ru-Yi Zhang [a, 1], Shi-Hua Luo [a, 1], Xiao-Min Lin [a], Xiu-Mei Hu [a], Ye Zhang [a], Xiao-He Zhang [a], Chang-Meng Wu [a], Lei Zheng [a, *], Qian Wang [a, b, **]

[a] Department of Laboratory Medicine, Nanfang Hospital, Southern Medical University, Guangzhou, 510515, Guangdong Province, PR China
[b] Department of Laboratory Medicine, Zhujiang Hospital, Southern Medical University, Guangzhou, 510280, Guangdong Province, PR China

HIGHLIGHTS

- A novel electrochemical biosensor for detection of exosomal miRNA is proposed.
- This electrochemical biosensor is based on step polymerization catalytic hairpin assembly (SP-CHA) circuit.
- This assembly exhibits great sensitivity and specificity for exosomal miR-181 detection.
- This assembly possesses great potential in cardiovascular disease diagnosis.

GRAPHICAL ABSTRACT

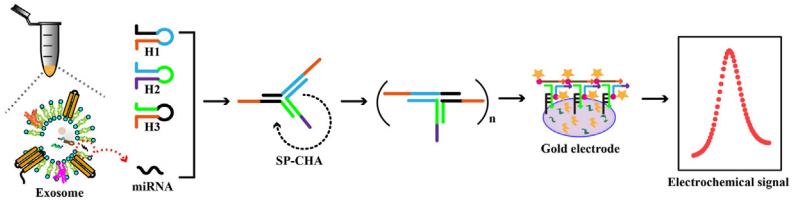

ARTICLE INFO

Article history:
Received 12 January 2021
Received in revised form
2 March 2021
Accepted 7 March 2021
Available online 14 March 2021

Keywords:
Electrochemical biosensor
Exosomal miRNA
Step polymerization catalytic hairpin assembly
Cardiovascular disease

ABSTRACT

Exosomal microRNAs (miRNAs) derived from different cells are proposed to be important noninvasive biomarkers for the diagnosis of cardiovascular disease. Recently, sensitive and reliable sensing of exosomal miRNAs has been garnered significant attention. Herein, a novel electrochemical biosensor based on a step polymerization catalytic hairpin assembly (SP-CHA) circuit is designed for exosomal miR-181 detection. Exosomal miR-181 as a trigger, induced SP-CHA process and generated a large number of T shaped concatemers with different length on the electrode surface. These ultra-concatemers could provide a much enhanced signal-to-noise ratio with the linear range from 10 fM to 100 nM and the detection limit of 7.94 fM. Furthermore, this assay was successfully applied to the detection of exosomal miR-181 in serum samples of normal healthy controls and patients with coronary heart disease (CHD) and the results were consistent with those analysis collected from qRT-PCR. The assembly demonstrated great performance in differentiating CHD patients from healthy controls (AUC:0.9867). Collectively, this sensing system possessed high stability and sensitivity with ease of operation and cost efficiency, leading to great potential for exosomal miRNAs detection in cardiovascular disease.

* Corresponding author.
** Corresponding author. Department of Laboratory Medicine, Nanfang Hospital, Southern Medical University, Guangzhou, 510515, Guangdong Province, PR China.
E-mail addresses: nfyyzhenglei@smu.edu.cn (L. Zheng), wangqian@smu.edu.cn (Q. Wang).
[1] These authors contributed equally to this work and should be considered co-first authors.

https://doi.org/10.1016/j.aca.2021.338396
0003-2670/

1. Introduction

The miRNAs are a group of small non-coding single-stranded RNAs of 19–23 nucleotides in length and specifically expressed in various types of cells and tissues, which functions in gene silencing and posttranscriptional regulation [1,2]. There is increasing recognition that miRNAs are closely associated with cardiovascular diseases. For instance, miRNAs including miRNA-21, miR-133, miR-296, and miR-181 were found in cardiomyocytes, which are associated with regulation of several biological processes in including heart development, cardiomyocytes apoptosis, heart arrhythmia, and heart failure [3,4]. Among these miRNAs, studies showed that miR-181 family members played an important role in myocyte death after ischemia [5]. In addition, miR-181 had been found highly expressed in exosomes secreted by cardiac macrophage to regulate reperfusion after myocardial infarction [6]. As such, miR-181 could serve as promising candidates of biomarkers for cardiovascular disease diagnosis.

Exosomes or extracellular vesicles (EVs) are small biological lipid membrane vesicles with diameters for 30–200 nm shed by all cell types into various body fluids [7], including the bloodstream [8,9]. Exosomes have been proven as an important medium for information exchange and disease development [10,11]. They convey intercellular communications by delivery of biomolecules, such as intact and functional miRNAs, messenger RNAs (mRNAs), and proteins [12,13]. Recently, an increasing number of extracellular miRNAs have been detected in exosomes isolated from biological fluids and cell culture media [14]. Exosomes are highly stable in biological fluids because the packaging in a lipid bilayer can prevent miRNAs from being degraded by humoral enzymes, resulting in a relatively long and stable expression duration [15]. Thus, to analyze the exosomal miRNAs has attracted much attention.

At present, various methods for exosomal miRNA detection have been reported. The most widely used assays include reverse transcription-polymerase chain reaction (RT-PCR) [16], digital PCR [17] and next-generation sequencing technology (NGS) [18]. Although these methods have excellent analytical performance, they are still suffering some defects for clinical applications. RT-PCR can be used for detecting exosomal miRNA, but it has a relatively low sensitivity and it relies on expensive equipment. Digital PCR can detect trace amounts of miRNA, but high cost and complex operation may restrict their further applications. NSG usually requires tedious pretreatment and complex processes. Therefore, an easy-to-operate assay with high sensitivity and specificity is needed for the assessment of exosomal miRNAs.

To circumvent these problems, electrochemical biosensor techniques, such as hybridization chain reaction (HCR), catalytic hairpin assembly (CHA), rolling circle amplification (RCA) and strand-displacement amplification (SDA) have become very powerful and attracted much attention [19–21]. Among these reactions, CHA is an enzyme-free, high-efficiency, and isothermal amplification method [22]. A typical CHA reaction is executed using two complementary DNA strands prepared as stable hairpin structures. Thus, spontaneous interaction between the two DNA strands is kinetically blocked, as the complementary domains are caged within the hairpin stems. With single-stranded nucleic acids, the two hairpins are opened successively because of the toehold nature, and the most thermodynamically favorable DNA duplexes are quickly formed [23]. CHA circuits function in the absence of enzymes under isothermal conditions, showing desirable amplification efficacy [24]. For this reason, CHA circuits have been adapted for the specific and sensitive detection of various targets like DNA, mRNA and miRNA in vitro or in living cells.

In the present work, we have developed a novel electrochemical biosensor based on a step polymerization catalytic hairpin assembly (SP-CHA) circuit for the analysis of exosomal miR-181. In this strategy, target miR-181 triggered and opened the hairpin H1 to start the SP-CHA reaction and self-elongated to generate accumulating three-way and T-shaped products. These products with different length help the immobilization of a large number of electrochemical species on the surface of the electrode and enhances the electrochemical response. This strategy offers a rapid, portable, disposable, enzyme-free, isothermal strategy to evaluate the signal of exosomal miR-181, leading to a promising and convenient platform for cardiovascular diseases.

2. Material and methods

2.1. Chemicals and reagents

All oligonucleotides used in our study were synthesized and purified by Sangon Biotechnology Co. Ltd. (Shanghai, China), and the detail sequences are listed in Table 1. .α-Naphthyl phosphate (α-NP), 6-mercapto-1-hexanol (MCH), bovine serum albumin (BSA), and streptavidin-alkaline phosphatase (ST-AP) were purchased from Sigma-Aldrich (St. Louis, MO, USA). 20 bp DNA Marker was purchased from TakaRa Biotech (Dalian, China). All other reagents were of analytical reagent grade. All aqueous solutions used in the experiments were prepared with Milli-Q water (≥18 MΩ, Milli-Q, Millipore). TE buffer (pH = 8.0) contained 10 mM Tris, 1 mM ethylenediaminetetraacetic acid (EDTA). Diethanolamine (DEA) buffer (pH = 9.6) contained 0.1 M DEA, 1 M $MgCl_2$ and 0.1 M KCl. Tris-HCl buffer used as washing buffer (pH = 7.40) contained 20 mM Tris, 0.1 M NaCl, 5.0 mM $MgCl_2$ and 0.05% Tween-20. Reaction buffer (pH = 7.40) contained 10 mM Tris, 0.1 mM NaCl, 5.0 mM $MgCl_2$.

2.2. Apparatus

All electrochemical measurements were performed on a CHI660E electrochemical workstation (Shanghai Chenhua Instruments Co. Ltd., China) with a conventional three-electrode system composed of platinum wire as the auxiliary, an Ag/AgCl electrode as the reference, a platinum electrode as the counter electrode and a 2 mm diameter gold electrode as the working electrode. Electrochemical measurements including electrochemical impedance spectroscopy (EIS), cyclic voltammetry (CV) and square wave voltammetry (SWV) were performed in 3 mL of 0.5 mM $K_3[Fe(CN)_6]$ solution. The EIS was conducted upon the application of 0.205 V biasing potential and 5 mV amplitude in the frequency range of 0.1 Hz–100 kHz. CV was scanned from +0.6 V to −0.2 V with a rate of 100 mV s^{-1}. The differential pulse voltammetry (DPV) measurements were carried out in 3 mL of DEA solution containing 1 mg mL^{-1} of α-NP substrate with the modulation time of 0.05 s, interval time of 0.017 s, step potential scan from 0.0 to + 0.6 V, and a standing time of 2 s. PAGE electrophoresis was performed on an electrophoresis analyzer (Bio-Rad, USA) and the gel was imaged on Gel Doc XR + system (Bio-Rad, USA).

2.3. Preparation of probes

All oligonucleotides were dissolved in TE buffer. Hairpin probes were designed based on the principle of an enzyme-free strand-displacement nucleic acid circuits system. The SP-CHA system consisted of three hairpin probes (H1, H2, H3), target probe (miR-181), capture probes on the surface of electrodes, and reaction buffer. In addition, H1 and H3 were covered with biotin labels. First, 10 μM H1, H2 and H3 were respectively denatured at 95 °C for 5 min, then cooled down 5 °C per minute to the room temperature and stored at 25 °C until used.

Table 1
DNA sequences of used in this assay.

Name	Sequence
Capture probe	5′−SH−TTTAGTCCAGCAACATATCACATAAC-3′
H1	5′- Biotin-ACCCACCGACAGCAATGAATGTTGAGAGAACCCGATATGAACATTCATTGCTGTCGA GACAAG-3′
H2	5′-TGAATGTTCATATCGGGTTCTCTCGGTGGGTCTTGTCTCGAGAGAACCCGATATGTTGCTGG ACT-3′
H3	5′- Biotin-GTTCTCTCGAGACAAGACCCACCAACATTCATTGCTGTCGGTGGGTCTTGTCTCGAC AGCAA-3′
Micro-181	5′-AACATTCATTGCTGTCGGTGGGT-3′
Mismatch 1(M1)	5′-AACATTCATTGCTGTC**C**GTGGGT-3′
Mismatch 2(M2)	5′-AACATTCATTGCTGT**GC**GTGGGT-3′
Mismatch 3(M3)	5′-AACATTCATTGCTG**AGC**GTGGGT-3′
Random RNA(R)	5′-TGGGTGGCTGTCGTTACTTACAA-3′

2.4. Preparation of electrochemical biosensor

The 2 mm bare gold electrode (Shanghai Chenhua Instruments Co. Ltd., China) was polished by 50 nM alumina slurries and treated in ultrapure water using ultrasound for a few minutes, and then soaked in piranha solution (H_2SO_4: H_2O_2 = 3:1) for 10 min to remove contaminants. The pretreated gold electrode was rinsed with Tris-HCl buffer and allowed to dry at room temperature. 10 μL of 0.2 μM thiolated capture probe was dropped onto the pretreated gold electrode surface and incubated overnight at 4 °C. After rinsing thoroughly with Tris-HCl buffer, the electrode was blocked into 10 μL of 1 mM MCH for 1 h at 25 °C. Afterwards, the electrode was further treated with the washing buffer and rinsed with 1% BSA for 30 min to block the non-specific binding sites on its surface and avoid the nonspecific adsorption of other oligonucleotides or enzymes. Then the electrochemical biosensor was obtained. H1, H2 and H3 were mixed with or without miR-181. After that, the modified electrode was incubated 10 μL of mixture with or without miR-181 (the terminal concentration of hairpin probes or miR-181 was 10 nM) at 25 °C. The SP-CHA products were hybridized with the capture probes immobilized on the gold electrode for 1 h.

Subsequently, the electrode was washed with DEA buffer containing 0.05% Tween-20, 10 μL of 0.9 μg mL^{-1} of ST-AP was dipped onto the electrochemical biosensor at 25 °C for 30 min, and washed thoroughly with DEA buffer containing 0.05% Tween-20.

2.5. PAGE electrophoresis

7 μL of SP-CHA products were mixed with 1.4 μL of 6 × loading buffer and analyzed by 12% native polyacrylamide gel electrophoresis (PAGE) in 0.5 × TBE buffer (89 mM tris-boric acid, 2 mM EDTA, pH = 8.3) at 140 V constant voltage for 40 min before staining with 4S red plus nucleic acid stain. The gels were visualized on a gel image system (Bio-Rad Laboratories, USA).

2.6. Clinical samples preparation and exosome isolation

Blood samples were collected from 15 patients with coronary heart disease (CHD) and 15 healthy controls (Nanfang Hospital, Southern Medical University). The diagnostic criteria of CHD include: the main blood vessels of the heart (left anterior descending coronary artery, circumflex artery and right coronary artery) have more than 50% stenosis. The clinical data of the individuals were shown in Supplemental Table 1. Blood samples were centrifuged at 3000 rpm at 4 °C for 10 min for serum collection, followed by an additional centrifugation step at 3000 g for 20 min and 10,000 g for 30min. 1 mL supernatants of different samples were collected for further exosome isolated by ultracentrifugation (UC) method. Transmission electron microscopy (TEM), Nanoparticle tracking analysis (NTA) and western blotting images were used to validate the characterization of exosomes.

2.7. Exosomal RNA isolation and quantitative validation by qRT-PCR

Exosomal total RNA was extracted by Hipure Serum/Plasma miRNA Mini Kit (Magen, R4314-03) according to the manufacturer's recommendations. Cel-miR-39 were used as exogenous standard control and added to co-isolated with exosomes. The final elution volume was 20 μL. And the RNA was quantified using nanodrop 2000C (Thermo Fisher Scientific, USA).

The reverse transcription reaction was carried out with Bulge-Loop™ miRNA qRT-PCR Starter Kit (Ribo, China) and the reaction system was incubated at 42 °C for 60 min and 70 °C for 10 min. The quantitative PCR amplification was performed with SYBR Green Dye detection (Takara, Japan) and the reaction was incubated in LightCycler 480 II (Roche, USA) as followed: (1) 95 °C for 10 min, (2) 95 °C for 2 s, 60 °C for 20 s, 70 °C for 10 s with 40 cycles. All the primers used here were designed by Ribo Biotechnology Co. Ltd. (Guangzhou, China).

3. Results and discussion

3.1. Design of the electrochemical biosensor

The SP-CHA system was composed of three hairpin probes (H1, H2, H3), target probe (miR-181), capture probes on the surface of electrodes and reaction buffer. The principle of our proposed SP-CHA strategy was illustrated in Scheme 1. SP-CHA involves two amplification pathway, seed generation and seed elongation. The seed generation process is actually a CHA reaction for three hairpin substrates (H1, H2, and H3). Being limited by a kinetic trap, assembly between the three hairpin substrates is too slow to happen. Only if target miR-181 (a 23-mer single stranded oligonucleotide) opens the first hairpin substrate (H1) through a toehold mediated strand displacement reaction will this process trigger two downstream strand displacement reactions. The middle segment of H1 (24 oligonucleotides) successively hybridizes with H2. Similarly, the middle segment of H2 (23 oligonucleotides) hybridizes with H3. Finally, a three-way and T-shaped assembly intermediate is formed. When the H1:H2:H3 assembly forms, it has two 16-base sticky ends long enough to hybridize with each other. Therefore, it can start self-elongation as a seed and finally form concatemer products of different lengths. Furthermore, H1 and H3 were modified with biotin labels. Finally, these biotinylated products can react with ST-AP and AP catalyzes the irreversible conversion of substrate α-NP to an electroactive product, generating an electrochemical signal that can be quantified by DPV.

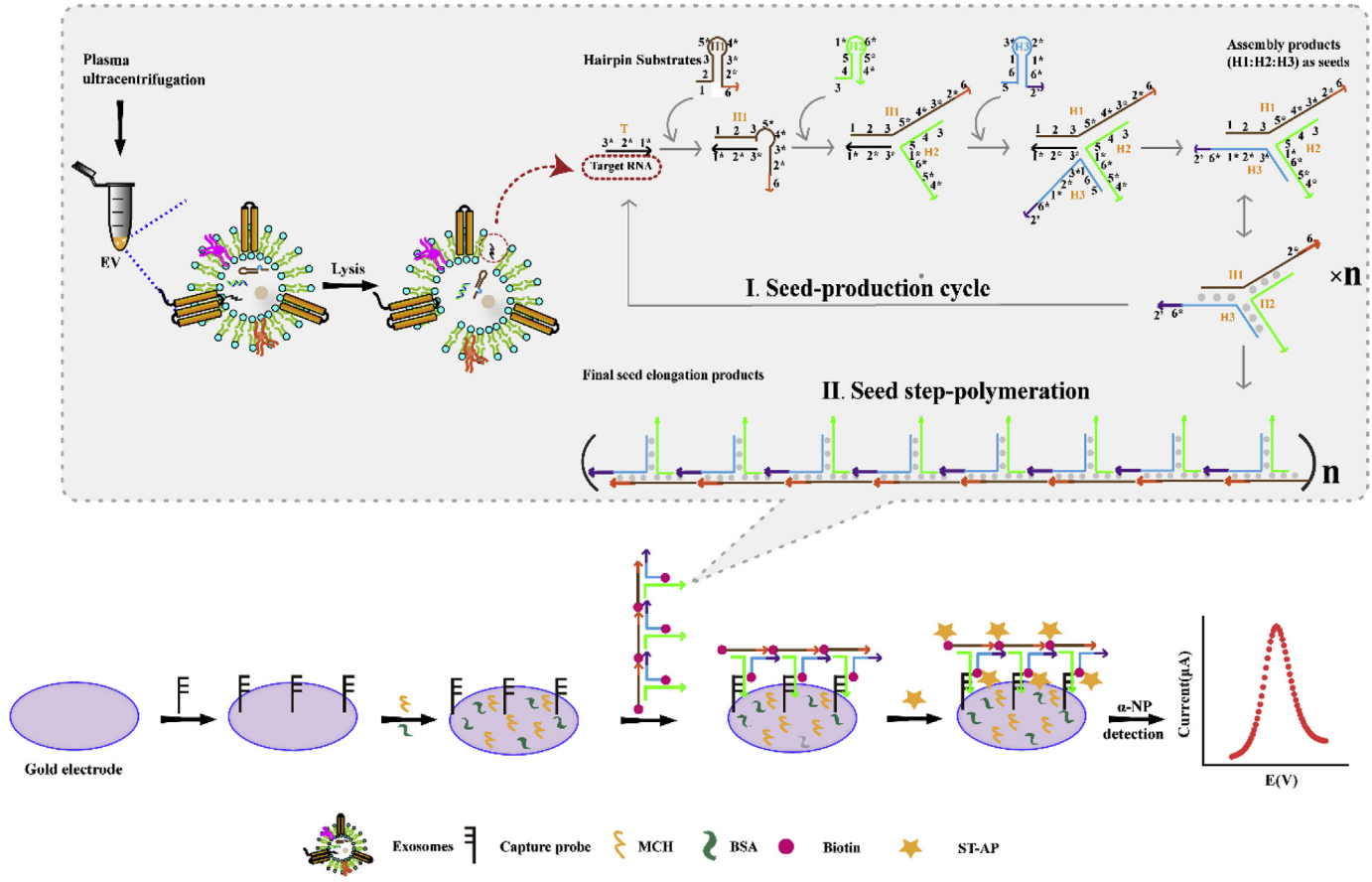

Scheme 1. Schematic illustration of the electrochemical sensor for detecting exosomal miRNA-181.

3.2. Validation of the CHA performance

The reaction principle of CHA was presented in Fig. 1A. The products and the sequences of the system were also investigated by PAGE. As shown in Fig. 1B, H1 (lane 1), H2 (lane 2) and H3 (lane3) were consistent with our design. In the absence of target probe, H1 could not hybridize with H2 (lane 5), and little H1, H2 and H3 complex was formed (lane 6). In the presence of target probe, the SP-CHA reaction was successfully performed, and self-elongation products with different length formed (lane 7). These results indicated that the SP-CHA led to remarkable signal amplification.

To verify the validity of the SP-CHA reaction, DPV measurements were also performed using different input probes. As shown in Fig. 1C–D, when the sensors were incubated without probes (blank, curve c), DPV peak current showed a very weak current signal. When H1, H2 and H3 was modified on the surface of electrode, the current increased a little (curve b). When target miR-181 and hairpin probes were both present, the SP-CHA was activated resulting in the enhanced signal output. The results indicated that the novel SP-CHA system could amplify the signal significantly and is feasible for downstream applications.

3.3. Characterization of the modified electrode

EIS, CV and SWV measurements were used to evaluate the modification of the electrochemical biosensor in each step. In EIS, the curve with a semicircular diameter was equal to the electron-transfer resistance (Ret). As showed in Fig. 2A, the bare electrode gave an almost straight line (curve a) because of electron free transfer, which reflected the outstanding electrochemical conductivity. When the capture probe was modified on the surface of electrode, the Ret increased slightly (curve b). This was because the negatively charged probes on the electrode surface led to electrostatic repulsion of $K_3[Fe(CN)_6]$. After modified of MCH and BSA, the Ret continually increased (curve c) because the biological molecules hindered the electron-transfer. The Ret continued to increase slightly when the remaining capture probe hybridized with the H1/H2/H3 complexes without the participation of the target probe (curve d). With the participation of the target probe, the Ret increased significantly (curve e), which indicated that only a few H1/H2/H3 can initiate the reaction in the absence of the target, and in the presence of the target miRNA catalyst, a large number of H1/H2/H3 complexes were obtained. The CV results and SWV measurements at different stages shown in Fig. 2B–C were in good agreement with those measured by EIS. Based on these results, the developed electrochemical biosensor was available.

3.4. Optimization of experimental conditions

The reaction time and temperature are important factors for the system. To achieve optimal detection performance, these important experimental parameters were investigated with 10 nM target probe and the concentration for H1/H2/H3 was 10 nM based on the pre-peer experiment. The signal-to-noise ratio was used to evaluate the performance of the biosensor. As seen in Fig. 3A, the signal-to-noise ratio went up with the increment of incubation time and reached the maximum at 1 h, demonstrating the optimized reaction time of target miRNA during CHA amplification was

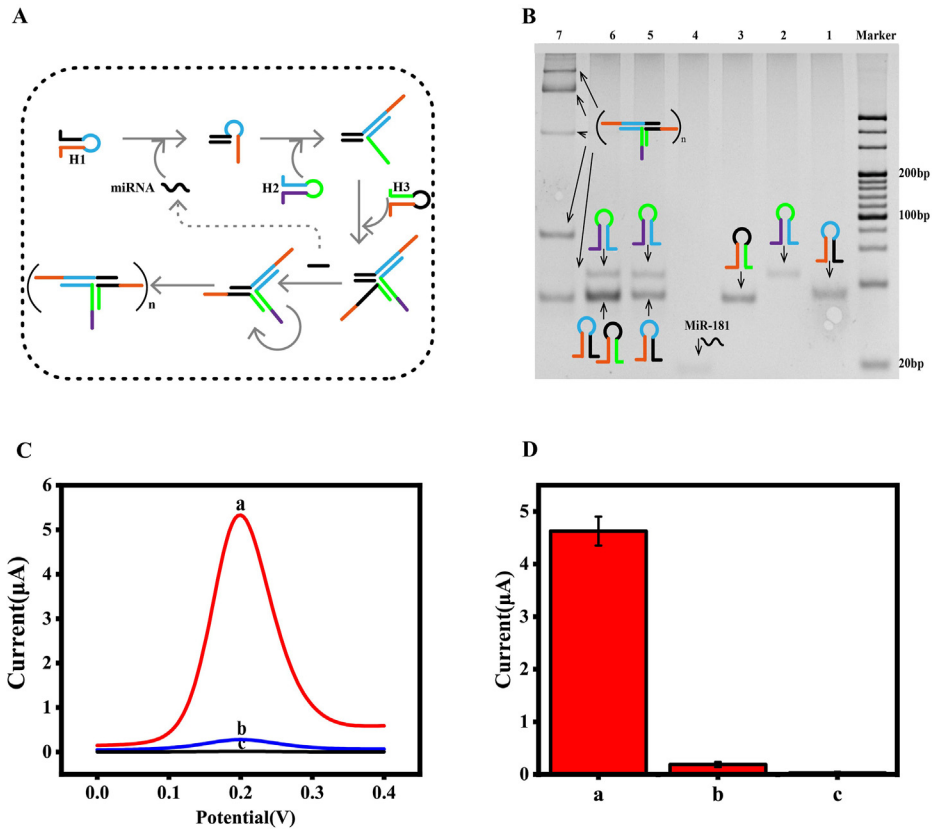

Fig. 1. **(A)** Schematic illustration of SP-CHA. **(B)** Native PAGE analysis of the SP-CHA products. Lane1: H1; Lane 2: H2; Lane 3: H3; Lane 4: miR181; Lane 5: H1+H2; Lane 6: H1+H2+H3; Lane 7: H1+H2+H3+miR181. The concentration of H1, H2, H3 and miR181 was 300 nM. **(C)** Typical DPV responses and **(D)** DPV peak currents under different conditions of (a) H1+H2+H3 (all were 10 nM) with 10 nM miR181; (b) H1+H2+H3 (all were 10 nM); (c) blank control (aqueous solution). The error bars represent standard deviations of the measurements (n = 3). The reaction temperature for SP-CHA was 25 °C and the incubation time was 60 min.

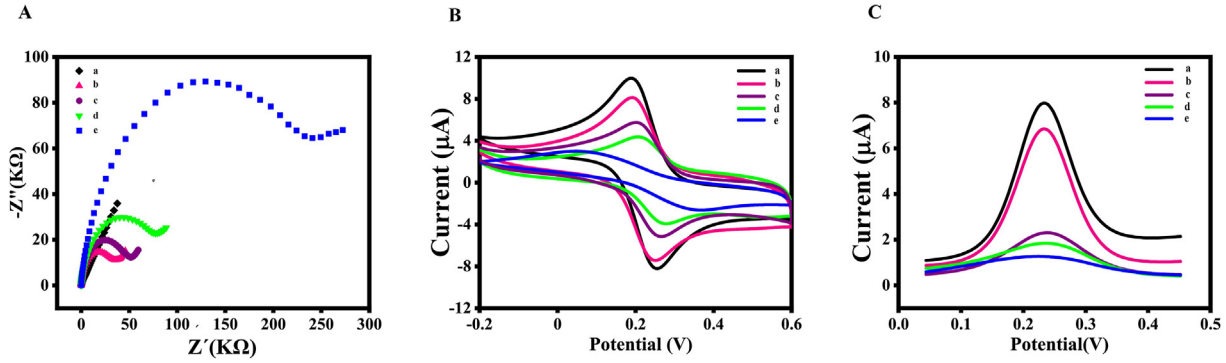

Fig. 2. EIS**(A)**, CV **(B)** and SWV **(C)** responses in 0.5 mM $[Fe(CN)_6]^{3-4-}$ solution containing 0.4 M KCl at different modification processes: (a) bare clectrode; (b) electrode modified by 10 μL of 0.2 μM capture probes; (c) 10 μL of 1 mM MCH and 1% BSA modified electrode; (d) 10 μL of 10 nM H1, H2, H3 complexes; (e) 10 μL of 10 nM miR181 hybridized with 10 nM H1, H2, H3 complexes.

1 h. In addition, the catalytic hairpin assembly process can be affected by the reaction temperature. The reaction temperature was examined from 4 °C to 42 °C, and the maximum signal-to-noise ratio was achieved at 25 °C (Fig. 3B). At low temperature, the low collision probability of the probes significantly reduced the formation of amplification products and increased non-specific biding. On the other hand, unstable hairpins would lead to a large number of nonspecific products. Therefore, 25 °C was chosen as the optimal reaction temperature.

3.5. Specificity of this assembly

We evaluated the specificity of the proposed electrochemical biosensor by detecting a blank control and four different kinds of control oligonucleotide: a single-base mismatched oligonucleotide, a double-base mismatched oligonucleotide, a triple-base mismatched oligonucleotide and a non-complementary oligonucleotide (random oligonucleotide). The DPV currents and DPV signal curves of these oligonucleotides were measured with a

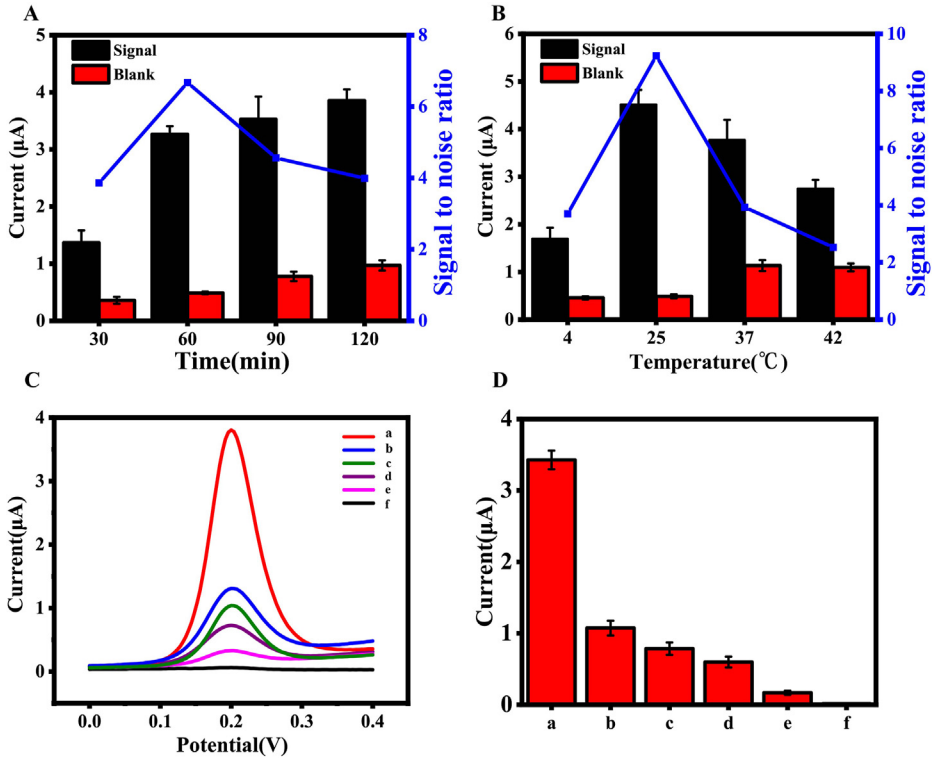

Fig. 3. The optimal reaction and specificity of the assembly. **(A–B)** Evaluation of effects of incubating time and temperature on the signal-to noise ratio, error bars represent standard deviations of the measurements (n = 3). **(C–D)** Typical DPV responses and DPV peak currents of 10 nM of different target: (a) miR181; (b) miR181 with single-base mismatch; (c) miR181 with double-base mismatch; (d) miR181 with triple-base mismatch; (e) random base; (f) blank control. The concentration of H1, H2, H3 for HCR was 10 nM and the reaction temperature was 25 °C and the incubation time was 60 min. The error bars represent standard deviations of the measurements (n = 3).

concentration of 10 nM under the optimized detection conditions. As can be seen in Fig. 3C–D, the DPV signal was decreased clearly in mismatched oligonucleotide compared with target miRNA. The peak current in different conditions were as follows: 3.57 μA for miRNA, 1.193 μA for single mismatch, 0.8757 μA for double mismatch, 0.6826 μA for triple mismatch, 0.1767 μA for random olignucleotide and 0.0205 μA for blank. It was easy to distinguish miRNA from mismatched or random oligonucleotide. In addition, the current signal was weak in oligonucleotides with three or more mismatched bases, which was comparable to that in blank solution. These results indicated that the current signal was specifically amplified by the target miRNA, suggesting that the SP-CHA electrochemical biosensor exhibited good performance for discriminating target miRNA from other oligonucleotides. Furthermore, biological interference of this method was studied by testing miRNA in reaction buffer and serum samples. As shown in Fig. S1, the DPV current peaks for testing two serum samples are nearly the same with the Tris-HCl performance with the same miRNA level. From the results, it is concluded that miRNA is stable in the biological samples with nearly no interference.

3.6. Analytical performance of miRNA detection

Under the optimum conditions of the experiment, the sensitivity of the prepared electrochemical biosensor was explored with different concentrations of target miRNA. As indicated in Fig. 4A, the DPV current signal gradually increased along with the increase of miRNA concentration and reached a maximum at the 100 nM. As shown in Fig. 4B, a good linear relationship between DPV current and the concentration of miRNA was observed in the range of 10 fM-100 nM; the linear regression equation was $i_p(\mu A) = 10.62 + 0.75105 \log C_{miR\text{-}181}$ (the unit is M), with a liner correlation coefficient of 0.9942. The detection limit of miRNA was estimated to be 7.94 fM based on the signal of blank tests and the standard deviation. As listed in Table 2, compared to other biosensors for the detection of exosomal miRNA [25–32], the linear range is relatively wide. Additionally, the detection time and sensitivity are also acceptable. Although imaging ellipsometry sensor and strategy with Ag nanoparticles have superior sensitivity, their complex operation and expensive facility may limit their clinical applications. In our work, the electrochemical biosensor with advantages included low cost, rapid detection, and easy to use will promote the advance of the point-of-care settings.

3.7. Detection in serum exosomal miRNA

3.7.1. The characterization of exosomes

According to International Society for Extracellular Vesicles (ISEV) guidelines, the exosomes were characterized [33]. At first, the serum exosomes from normal healthy controls (NC) or CHD patients were examined by TEM. The harvested serum exosomes were saucer-like and about mean diameter of 100 nm (Fig. 5A), which was consistent with the characteristics of exosomes reported in the previously literature [34]. Subsequently, the identity of the exosomes was validated through detection of CD9, CD63 and TSG101 [35]. From Fig. 5B, the western blotting (WB) images validated that there were abundant CD9, CD81, and TSG101 in serum exosomes from both groups. Furthermore, we used NTA to quantify exosomes concentration and average diameter. As illustrated in Fig. 5C, the concentration of the collected exosomes was 6.21×10^8 (NC) and 1.12×10^8 (CHD) particles mL^{-1}, and the average diameter was 131.9 (NC) and 79.4 (CHD) nm, which is consistent with

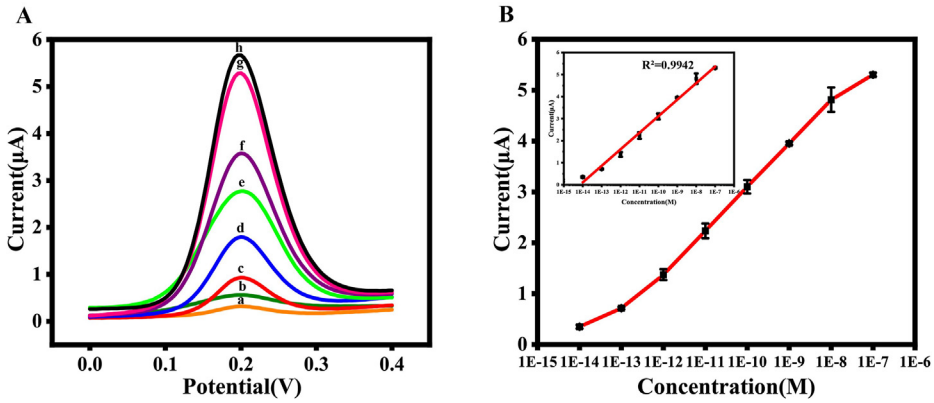

Fig. 4. **(A)** DPV responses and **(B)** The calibration curve of the electrochemical biosensor to different concentrations of miR181. From a to h: 10 fM, 100 fM, 1 pM, 10 pM, 100 pM, 1 nM, 10 nM, and 100 nM. The error bars represent standard deviations of the measurements (n = 3).

Table 2
Comparison of different detecting biosensors for miRNAs.

Strategy	Technique	Reaction time	Detection range	LOD	Ref
hybridization chain reaction with DNAzyme	Fluorescence	120 min	10 pM-10 nM	10 pM	[25]
Magnetic beads pre-functionalized with capture probes	Electrochemical	100 min	1 pM-10 nM	1 pM	[26]
Tetrahedron DNA probes targeted with miRNA to form DNA hydrogelation on Au film	Imaging ellipsometry senor	Not given	0.2 fM-100 nM	0.2 fM	[27]
Signal amplification strategy based on the deposition of AgNPs	Electrochemical	255 min	1 fM-200 pM	0.4 fM	[28]
Ratiometric electrochemical DNA based on a locked nucleic acid-modified structure	Electrochemical	Not given	10 fM-70 fM	2.3 fM	[29]
Rolling circular amplification with CRISPR/Cas system	Fluorescence	190 min	1 pM-10 nM	90 fM	[30]
Photonic crystal barcodes with hybridization chain reaction	Fluorescence	240 min	1 nM-10 μM	1 nM	[31]
Switching the visible-light-induced oxidase mimic activity of acridone derivate with duplex-strand specific nuclease	Colorimetric biosensor	185 min	50 fM-3 pM	44.76 fM	[32]
step polymerization catalytic hairpin assembly	Electrochemical	180 min	10 fM-100 nM	7.94 fM	This work

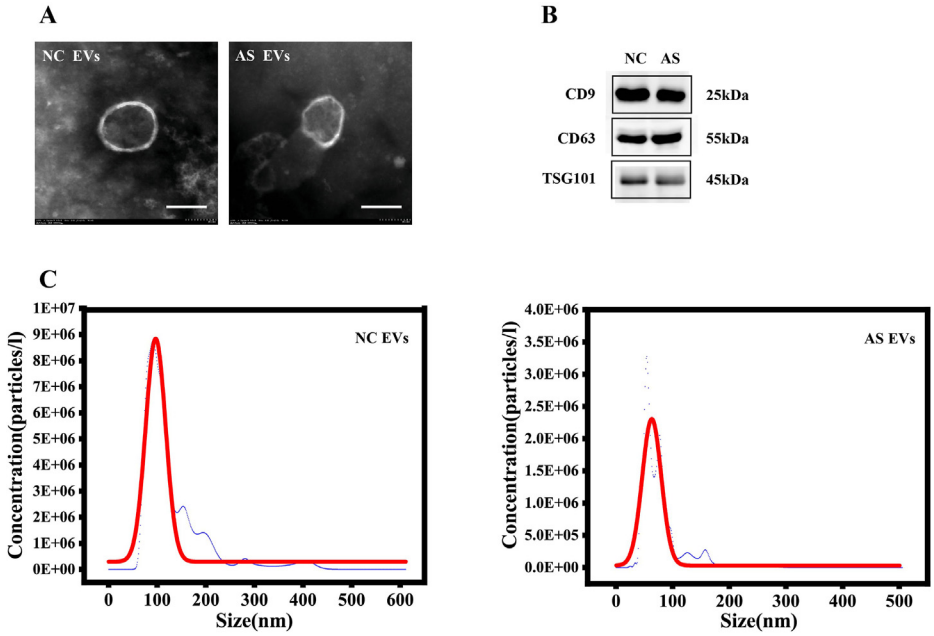

Fig. 5. Characterization of isolated exosomes from serum of healthy controls and CHD patients. **(A)** TEM of exosomes from serum of normal healthy controls and atherosclerosis patients. Scale bars = 200 nm. **(B)** WB images for CD9, CD63 and TSG101 in exosomes from serum of normal healthy controls and atherosclerosis patients. **(C)** Size and size distribution of the exosomes from serum of normal healthy controls and atherosclerosis patients as analyzed by NTA.

previous report [36].

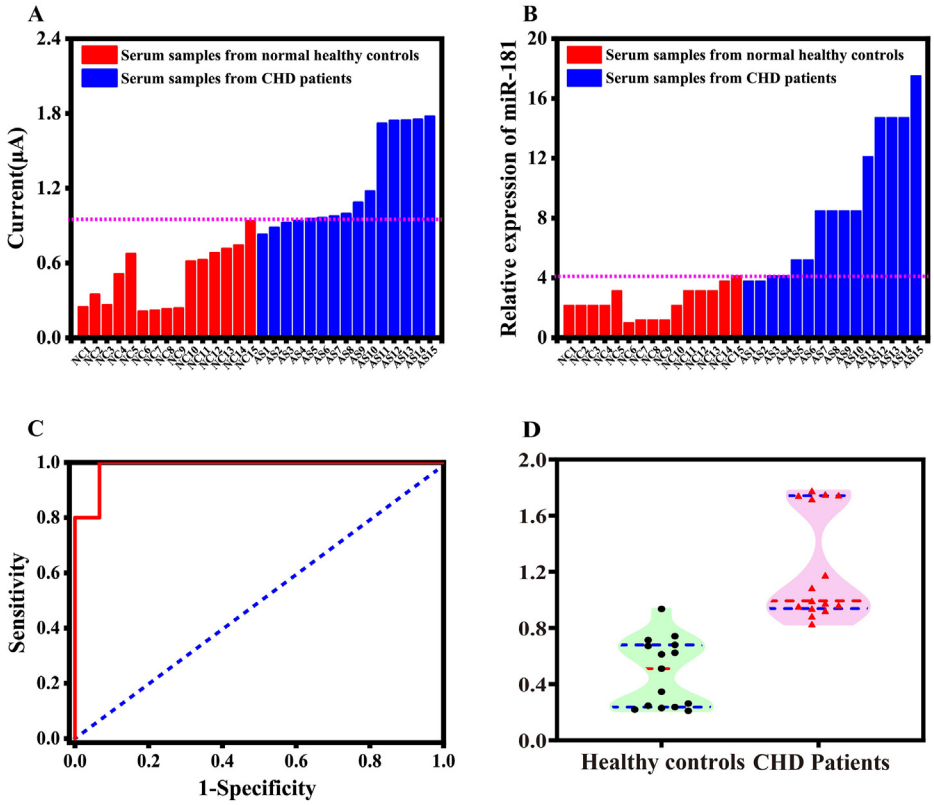

Fig. 6. **(A)** DPV peak currents of the sensor to 2 μl RNA of exosomes extracted from 1 mL serum sample of normal healthy controls or atherosclerosis patients (both n = 15). The concentration of H1, H2, H3 for SP-CHA was 10 nM and the reaction temperature was 25 °C and the incubation time was 60 min. **(B)** The relative expression of exosomal miR181 in serum between NC group and CHD group were calculated as $2^{-\triangle Ct}$, and $\triangle Ct = AvgCt_{miR181}$- $AvgCt_{cel\text{-}miR\text{-}39}$. And the results were normalized. **(C)** ROC curve of DPV signals of serum exosomal miR181. **(D)** Violin plot analysis comparing the levels and distributions of DPV responses in healthy controls and CHD patients.

3.7.2. Detection of miRNA-181 in serum exosomes

The biosensor was also used to detect miRNA-181 in serum exosomes from 15 normal healthy controls and 15 CHD patients. As shown in Fig. 6A, the range of current in NC samples was from 0.21 μA to 0.94 μA while the data in CHD patients was from 0.83 μA to 1.78 μA. Then, we used qRT-PCR to measure the Ct value of exosomal miR-181, in which cel-miR-39 was acted as an exogenous standard control. The average Ct for each triplicate from qRT-PCR was calculated, the relative expression of exosomal miR-181 between NC group and CHD group were calculated as $2^{-\triangle Ct}$, and $\triangle Ct = AvgCt_{miR\text{-}181}$- $AvgCt_{cel\text{-}miR\text{-}39}$. As shown in Fig. 6B, the results of the proposed biosensor were performed in parallel to those of qRT-PCR. Additionally, ROC of SP-CHA indicated that AUC could be up to 0.9867 with 93.33% sensitivity and 93.33% specificity (Fig. 6C), demonstrating that our biosensor performed high accuracy and practical value. Moreover, we conducted violin plot analysis to compare the DPV responses in both groups. The results indicated that the DPV signals in both groups showed bimodal patterns. Meanwhile, a low current signal was detected in all healthy individuals, whereas the DPV responses increased significantly in CHD patients. Furthermore, to compare the sensitivity and specificity between qRT-PCR and SP-CHA method, standard miR-181 was used to construct absolute calculation. The standard curve of qRT-PCR was shown in Fig. S2. And Fig. S3 indicated that AUC for qRT-PCR could be up to 0.9956 with 86.67% sensitivity and 100.00% specificity. The results showed that compared to qRT-PCR, SP-CHA method had a higher sensitivity.

4. Conclusion

In a short, we have developed a simple and specific electrochemical biosensor for detection of exosomal miR-181 using binding-induced SP-CHA. This assembly exhibited excellent analytical performance, allowing a lot of AP enzymes to be captured, which led to significant enhancement of the final electrochemical signal. The biosensor exhibits high sensitivity with low detection limit of 7.94 fM and high specificity with even single base mismatch sequence. Furthermore, the levels of miRNA-181 in serum exosome tested by this method were in excellent consistence with qRT-PCR, with a sensitivity of 99.33% and a specificity of 99.33%. Consequently, we envision this proposed biosensor can be acted as a potentially tool for the accurate detection of exosome miRNA analysis in cardiovascular diseases.

CRediT authorship contribution statement

Ru-Yi Zhang: Conceptualization, Methodology, Writing – original draft. **Shi-Hua Luo:** Data curation, Investigation, Software, Validation. **Xiao-Min Lin:** Data curation, Visualization, Investigation. **Xiu-Mei Hu:** Writing – review & editing. **Ye Zhang:** Software, Writing – review & editing. **Xiao-He Zhang:** Data curation, Software, Validation. **Chang-Meng Wu:** Data curation. **Lei Zheng:** Supervision. **Qian Wang:** Conceptualization, Supervision.

Declaration of competing interest

The authors declare that they have no known competing financial interests or personal relationships that could have appeared to influence the work reported in this article.

Acknowledgements

This work was supported by the National Natural Science Foundation of China (grant numbers: 81772244, 82072334).

Appendix A. Supplementary data

Supplementary data to this article can be found online at https://doi.org/10.1016/j.aca.2021.338396.

References

[1] D.P. Bartel, MicroRNAs: genomics, biogenesis, mechanism, and function, Cell 116 (2004) 281–297, https://doi.org/10.1016/s0092-8674(04)00045-5.
[2] T.S. Elton, H. Selemon, S.M. Elton, N.L. Parinandi, Regulation of the MIR155 host gene in physiological and pathological processes, Gene 532 (2013) 1–12, https://doi.org/10.1016/j.gene.2012.12.009.
[3] J.M. Moon, L. Xu, R.G. Giffard, Inhibition of microRNA-181 reduces forebrain ischemia-induced neuronal loss, J. Cerebr. Blood Flow Metabol. 33 (2013) 1976–1982, https://doi.org/10.1038/jcbfm.2013.157.
[4] X. Wang, X. Zhang, X.P. Ren, J. Chen, H.Z. Liu, J.Q. Yang, M. Medvedovic, Z.W. Hu, G.C. Fan, MicroRNA-494 targeting both proapoptotic and anti-apoptotic proteins protects against ischemia/reperfusion-induced cardiac injury, Circulation 122 (2010) 1308–1318, https://doi.org/10.1161/CIRCULATIONAHA.110.964684.
[5] S. Das, M. Kohr, B. Dukerly-Eyring, D.I. Lee, D. Bedja, O.A. Kent, A.K. Leung, J. Henao-Mejia, R.A. Flavell, C. Steenbergen, Divergent effects of miR-181 family members on myocardial function through protective cytosolic and detrimental mitochondrial microRNA targets, J Am Heart Assoc 6 (2017), e004694, https://doi.org/10.1161/JAHA.116.004694.
[6] G. de Couto, R. Gallet, L. Cambier, E. Jaghatspanyan, N. Makkar, J.F. Dawkins, B.P. Berman, E. Marbán, Exosomal MicroRNA transfer into macrophages mediates cellular postconditioning, Circulation 136 (2017) 200–214, https://doi.org/10.1161/CIRCULATIONAHA.116.024590.
[7] E.G. Trams, C.J. Lauter, J. Norman Salem, U. Heine, Exfoliation of membrane ecto-enzymes in the form of micro-vesicles, Biochim. Biophys. Acta 645 (1981) 63–70, https://doi.org/10.1016/0005-2736(81)90512-5.
[8] G. Raposo, W. Stoorvogel, Extracellular vesicles: exosomes, microvesicles, and friends, J. Cell Biol. 200 (2013) 373–383, https://doi.org/10.1146/annurev-biochem-013118-111902.
[9] D.M. Pegtel, S.J. Gould, Exosomes, Annu. Rev. Biochem. 88 (2019) 487–514, https://doi.org/10.1083/jcb.201211138.
[10] C. He, S. Zheng, Y. Luo, B. Wang, Exosome theranostics: biology and translational medicine, Theranostics 8 (2018) 237–255, https://doi.org/10.7150/thno.21945.
[11] D.G. Meckes Jr., K.H. Shair, A.R. Marquitz, C.P. Kung, R.H. Edwards, N. Raab-Traub, Human tumor virus utilizes exosomes for intercellular communication, Proc. Natl. Acad. Sci. U. S. A. 107 (2010) 20370–20375, https://doi.org/10.1073/pnas.1014194107.
[12] Y. Zhou, G. Zhou, C. Tian, W. Jiang, L. Jin, C. Zhang, X. Chen, Exosome-mediated small RNA delivery for gene therapy, Wiley Interdiscip. Rev. RNA 7 (2016) 758–771, https://doi.org/10.1002/wrna.1363.
[13] S. Fang, C. Xu, Y. Zhang, C. Xue, C. Yang, H. Bi, X. Qian, M. Wu, K. Ji, Y. Zhao, Y. Wang, H. Liu, X. Xing, Umbilical cord-derived mesenchymal stem cell-derived exosomal MicroRNAs suppress myofibroblast differentiation by inhibiting the transforming growth factor-β/SMAD2 pathway during wound healing, Stem Cells Transl. Med. 5 (2016) 1425–1439, https://doi.org/10.5966/sctm.2015-0367.
[14] H. Valadi, K. Ekström, A. Bossios, M. Sjöstrand, J.J. Lee, J.O. Lötvall, Exosome-mediated transfer of mRNAs and microRNAs is a novel mechanism of genetic exchange between cells, Nat. Cell Biol. 9 (2007) 654–659, https://doi.org/10.1038/ncb1596.
[15] Y. Chen, Y. Song, J. Huang, M. Qu, Y. Zhang, J. Geng, Z. Zhang, J. Liu, G.Y. Yang, Increased circulating exosomal miRNA-223 is associated with acute ischemic stroke, Front. Neurol. 8 (2017), https://doi.org/10.3389/fneur.2017.00057.
[16] K. Rekker, M. Saare, A.M. Roost, A.L. Kubo, N. Zarovni, A. Chiesi, A. Salumets, M. Peters, Comparison of serum exosome isolation methods for microRNA profiling, Clin. Biochem. 47 (2014) 135–138, https://doi.org/10.1016/j.clinbiochem.2013.10.020.
[17] C. Wang, Q. Ding, P. Plant, M. Basheer, C. Yang, E. Tawedrous, A. Krizova, C. Boulos, M. Farag, Y. Cheng, G.M. Yousef, Droplet digital PCR improves urinary exosomal miRNA detection compared to real-time PCR, Clin. Biochem. 67 (2019) 54–59, https://doi.org/10.1016/j.clinbiochem.2019.03.008.
[18] L. Zhang, C. Hao, S. Yao, R. Tang, W. Guo, H. Cong, J. Li, L. Bao, D. Wang, Y. Li, X. Yu, S. Duan, W. Yao, Exosomal miRNA profiling to identify nanoparticle phagocytic mechanisms, Small 14 (2018), e1704008, https://doi.org/10.1002/smll.201704008.
[19] X. Li, X. Li, D. Li, M. Zhao, H. Wu, B. Shen, P. Liu, S. Ding, Electrochemical biosensor for ultrasensitive exosomal miRNA analysis by cascade primer exchange reaction and MOF@Pt@MOF nanozyme, Biosens. Bioelectron. 168 (2020) 112554, https://doi.org/10.1016/j.bios.2020.112554.
[20] P. Miao, Y. Tang, Dumbbell hybridization chain reaction based electrochemical biosensor for ultrasensitive detection of exosomal miRNA, Anal. Chem. 92 (2020) 12026–12032, https://doi.org/10.1021/acs.analchem.0c02654.
[21] X. Tang, Y. Wang, L. Zhou, W. Zhang, S. Yang, L. Yu, S. Zhao, K. Chang, M. Chen, Strand displacement-triggered G-quadruplex/rolling circle amplification strategy for the ultra-sensitive electrochemical sensing of exosomal microRNAs, Mikrochim. Acta 187 (2020) 172, https://doi.org/10.1007/s00604-020-4143-9.
[22] B. Li, A.D. Ellington, X. Chen, Rational, modular adaptation of enzyme-free DNA circuits to multiple detection methods, Nucleic Acids Res. 39 (2011) e110, https://doi.org/10.1093/nar/gkr504.
[23] Q. Li, F.P. Zeng, N. Lyu, J. Liang, Highly sensitive and specific electrochemical biosensor for microRNA-21 detection by coupling catalytic hairpin assembly with rolling circle amplification, Analyst 143 (2018) 2304–2309, https://doi.org/10.1039/c8an00437d.
[24] J. Liu, Y. Zhang, H. Xie, L. Zhao, L. Zheng, H. Ye, Applications of catalytic hairpin assembly reaction in biosensing, Small 15 (2019), e1902989, https://doi.org/10.1002/smll.201902989.
[25] K. Boriachek, M. Umer, M.N. Islam, V. Gopalan, A.K. Lam, N.T. Nguyen, M.J.A. Shiddiky, An amplification-free electrochemical detection of exosomal miRNA-21 in serum samples, Analyst 143 (2018) 1662–1669, https://doi.org/10.1039/c7an01843f.
[26] D. He, L. Hai, H. Wang, R. Wu, H.W. Li, Enzyme-free quantification of exosomal microRNA by the target-triggered assembly of the polymer DNAzyme nanostructure, Analyst 143 (2018) 813–816, https://doi.org/10.1039/c7an01691c.
[27] W. Cheng, J. Ma, P. Cao, Y. Zhang, C. Xu, Y. Yi, J. Li, Enzyme-free electrochemical biosensor based on double signal amplification strategy for the ultra-sensitive detection of exosomal microRNAs in biological samples, Talanta 219 (2020) 121242, https://doi.org/10.1016/j.talanta.2020.121242.
[28] L. Luo, L. Wang, L. Zeng, Y. Wang, Y. Weng, Y. Liao, T. Chen, Y. Xia, J. Zhang, J. Chen, A ratiometric electrochemical DNA biosensor for detection of exosomal MicroRNA, Talanta 207 (2020) 120298, https://doi.org/10.1016/j.talanta.2019.120298.
[29] R. Wang, X. Zhao, X. Chen, X. Qiu, G. Qing, H. Zhang, L. Zhang, X. Hu, Z. He, D. Zhong, Y. Wang, Y. Luo, Rolling circular amplification (RCA)-Assisted CRISPR/Cas9 cleavage (RACE) for highly specific detection of multiple extracellular vesicle MicroRNAs, Anal. Chem. 92 (2020) 2176–2185. http://10.1021/acs.analchem.9b04814.
[30] X. Wei, F. Bian, X. Cai, Y. Wang, L. Cai, J. Yang, Y. Zhu, Y. Zhao, Multiplexed detection strategy for bladder cancer MicroRNAs based on photonic crystal barcodes, Anal. Chem. 92 (2020) 6121–6127, https://doi.org/10.1021/acs.analchem.0c00630.
[31] L. Zou, Z. Wu, X. Liu, Y. Zheng, W. Mei, Q. Wang, X. Yang, K. Wang, DNA hydrogelation-enhanced imaging ellipsometry for sensing exosomal microRNAs with a tunable detection range, Anal. Chem. 92 (2020) 11953–11959, https://doi.org/10.1021/acs.analchem.0c02345.
[32] Y. Xia, T. Chen, L. Zhang, X. Zhang, W. Shi, G. Chen, W. Chen, J. Lan, C. Li, W. Sun, J. Chen, Colorimetric detection of exosomal microRNA through switching the visible-light-induced oxidase mimic activity of acridone derivate, Biosens. Bioelectron. 173 (2021) 112834, https://doi.org/10.1016/j.bios.2020.112834.
[33] J. Lötvall, A.F. Hill, F. Hochberg, E.I. Buzás, D. Di Vizio, C. Gardiner, Y.S. Gho, I.V. Kurochkin, S. Mathivanan, P. Quesenberry, S. Sahoo, H. Tahara, M.H. Wauben, K.W. Witwer, C. Théry, Minimal experimental requirements for definition of extracellular vesicles and their functions: a position statement from the International Society for Extracellular Vesicles, J. Extracell. Vesicles 3 (2014) 26913, https://doi.org/10.3402/jev.v3.26913.
[34] J. Zhang, L.L. Wang, M.F. Hou, Y.K. Xia, W.H. He, A. Yan, Y.P. Weng, L.P. Zeng, J.H. Chen, A ratiometric electrochemical biosensor for the exosomal microRNAs detection based on bipedal DNA walkers propelled by locked nucleic acid modified toehold mediate strand displacement reaction, Biosens. Bioelectron. 102 (2018) 33–40, https://doi.org/10.1016/j.bios.2017.10.050.
[35] C. Théry, K.W. Witwer, E. Aikawa, M.J. Alcaraz, J.D. Anderson, R. Andriantsitohaina, A. Antoniou, T. Arab, F. Archer, G.K. Atkin-Smith, D.C. Ayre, J.M. Bach, D. Bachurski, H. Baharvand, L. Balaj, S. Baldacchino, N.N. Bauer, A.A. Baxter, M. Bebawy, C. Beckham, A. Bedina Zavec, A. Benmoussa, A.C. Berardi, P. Bergese, E. Bielska, C. Blenkiron, S. Bobis-Wozowicz, E. Boilard, W. Boireau, A. Bongiovanni, et al., Minimal information for studies of extracellular vesicles 2018 (MISEV2018): a position statement of the International Society for Extracellular Vesicles and update of the MISEV2014 guidelines, J. Extracell. Vesicles 7 (2018) 1535750, https://doi.org/10.1080/20013078.2018.1535750.
[36] E.A. Kwizera, R. O'Connor, V. Vinduska, M. Williams, E.R. Butch, S.E. Snyder, X. Chen, X. Huang, Molecular detection and analysis of exosomes using surface-enhanced Raman scattering gold nanorods and a miniaturized device, Theranostics 8 (2018) 2722–2738, https://doi.org/10.7150/thno.21358.